On the modelling of temperature dependence of subthreshold swing in MOSFETs down to cryogenic temperature

Gérard Ghibaudo, Mohamed Aouad, Mikaël Cassé, Sebastien Martinie, Francis Balestra, Thierry Poiroux

On the modelling of temperature dependence of subthreshold swing in MOSFETs down to cryogenic temperature

G. Ghibaudo[1], M. Aouad[2], M. Casse[2], S. Martinie[2], T. Poiroux[2], F. Balestra[1]

1) IMEP-LAHC, Université Grenoble Alpes, MINATEC/INPG, 38016, Grenoble (France)
2) LETI-CEA, Université Grenoble Alpes, MINATEC, 38054 Grenoble (France)
Email: ghibaudo@minatec.inpg.fr

Abstract

A comprehensive analysis of the MOSFET subthreshold swing for a 2D subband with exponential band tail of states is first proposed. Then, a compact analytical expression for the subthreshold swing as a function of temperature is derived, well accounting for both its cryogenic temperature saturation and classical higher temperature increase. Moreover, a generalized subthreshold swing calculation applicable to the situation where the MOSFET drain current should be evaluated from the conductivity function within the Kubo-Greenwood formalism is developed.

1. Introduction

Cryogenic CMOS electronics is still an active research area as enabling circuit performance improvements in terms of operation speed, turn-on behaviour, thermal noise reduction, punch-through current decrease… [1-5]. Cryoelectronics finds application in high speed classical computing, sensing and detection, space electronics and more recently on readout CMOS for quantum computing [6,7]. In this context, the subthreshold swing, $SS=dV_g/dLn(I_d)$, V_g being the gate voltage, is a key parameter measuring the turn-on capability of the MOSFET. Recently, it has been shown that the saturation of the subthreshold swing at cryogenic temperatures could originate from an exponential tail of states at the 2D subband edge [8,9].

In this work, we first propose a comprehensive analysis of the MOSFET subthreshold swing for a single 2D subband with exponential band tail of states, and, we derive a compact analytical expression for the subthreshold swing as a function of temperature, well accounting for both its cryogenic temperature saturation and classical higher temperature increase. Moreover, we generalize the subthreshold swing derivation to the more realistic case where the drain current is calculated from the conductivity function (and not simply from the carrier DOS) within the Kubo-Greenwood formalism.

2. Modelling of MOSFET Subthreshold swing

2.1. Carrier density approach

First, following [8,9], we assume that the drain current Id is proportional to the inversion layer carrier density n and that the carrier mobility is a constant, such that $SS \equiv dV_g/dLn(I_d)=dV_g/dLn(n)$.

As is usual, the 2D carrier density n is calculated using the Fermi-Dirac statistics as:

$$n(E_f,T) = \int_{-\infty}^{+\infty} N(E,\Delta E).f(E,E_f)dE \tag{1}$$

where $f(E,E_f)=1/[1+e^{(E-Ef)/kT}]$ is the Fermi-Dirac function, E_f the Fermi level, T the temperature and k the Boltzmann constant. For a 2D subband, the energy density of states (DOS) $N(E,\Delta E)$ with exponential band tail (see Fig. 1) can be equated to:

$$N(E,\Delta E) = \frac{A_{2D}}{1+\exp\left(-E/\Delta E\right)} \tag{2}$$

with ΔE the band tail extension, $A_{2D}=g.m_d^*/(\pi.h_b)$ the 2D density of states with g the subband degeneracy factor, m_d^* the DOS effective mass and h_b reduced the Planck's constant. Note that, contrary to [9, Eq. 1], Eqs (1-2) well account also for the states situated above the band edge (here $E_c=0$). Note also that this exponential band tail finds its origin in potential-fluctuation-induced disorder with transport taking place by percolation [10].

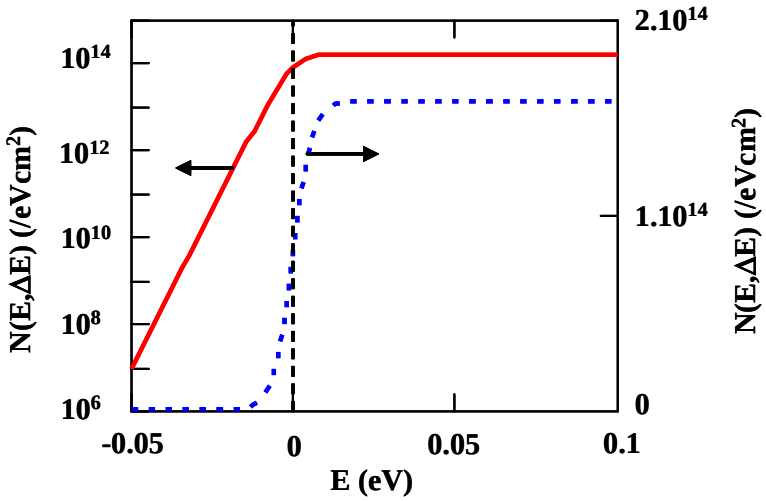

Fig. 1. 2D subband density of states with exponential tail (E=0 corresponds to band edge E_c, ΔE=3meV).

In weak inversion (WI), where the subthreshold swing is evaluated, the carrier density can be neglected in the MOS gate charge conservation equation, such that,

$$V_g \approx V_{fb} + V_s + \frac{Q_d(V_s)}{C_{ox}} + \frac{C_{it}.(V_s - V_0)}{C_{ox}} \qquad \text{(WI)} \tag{3}$$

where Q_d is the depletion charge, V_s the surface potential, V_{fb} the flat band voltage, V_0 channel Fermi potential, C_{ox} the gate oxide capacitance and C_{it}=q.N_{it} the interface trap capacitance. Since, the Fermi level E_f varies linearly with V_s, the subthreshold swing can be derived as,

$$SS = \frac{dV_g}{dLn(n)} = \frac{dV_g}{dV_s}.\frac{dV_s}{dLn(n)} = \frac{dV_g}{dV_s}.\frac{n}{q}.\frac{dE_f}{dn} \tag{4}$$

Using Eqs (1) and (3) yields for the subthreshold swing the general expression,

$$SS(T) = \frac{1}{q}.\frac{\int_{-\infty}^{+\infty} N(E,\Delta E).f(E,E_f)dE}{\int_{-\infty}^{+\infty} N(E,\Delta E).\left(-\frac{\partial f}{\partial E}\right)(E,E_f)dE}.\frac{C_{ox}+C_d+C_{it}}{C_{ox}} \tag{5}$$

where C_d=dQ_d/dV_s is the depletion capacitance (or without loss of generality the coupling capacitance between the inversion channel and the body contact for FDSOI structure i.e. C_d=C_{si}.C_{box}/(C_{box}+C_{si}), C_{si} being the silicon film capacitance and C_{box} the back oxide capacitance).

Then, it is easy to show from Eq. (5) that, in weak inversion where n<<kT.A_{2D} (≈10^{10}/cm^2 at T=4.2K, here n=10^7/cm^2), the subthreshold swing reduces respectively to,

$$SS(T) \approx \frac{kT_S}{q}.\frac{C_{ox}+C_d+C_{it}}{C_{ox}} \tag{6a}$$

for degenerate statistics when T<<T_S (with kT_S=ΔE) and to,

$$SS(T) = \frac{kT}{q}.\frac{C_{ox}+C_d+C_{it}}{C_{ox}} \qquad (6b)$$

for Boltzmann's statistics when $T>>T_S$.

Typical variations of SS with temperature are illustrated in Fig. 2, showing the saturation at low temperature ($T<T_S$) and the Boltzmann linear trend at high temperature ($T>T_S$). This behavior simply means that, at high temperature ($T>T_S$), the band tail has a negligible influence on the whole DOS, whereas, at low temperature ($T<T_S$), the band tail dominates the DOS in the carrier density calculation with degenerate statistics.

As can be seen from Fig. 2 and as suggested from Eqs (6), these variations with temperature of the subthreshold swing can be very well fitted by the empirical closed-form expression given by Eq. (7):

$$SSanal(T) = \frac{kT_S}{q}.\frac{C_{ox}+C_d+C_{it}}{C_{ox}}.\left[1+\alpha.Ln\left(1+e^{\frac{T-T_S}{\alpha T_S}}\right)\right] \qquad (7)$$

where α is a smoothing parameter (here ≈ 0.1).

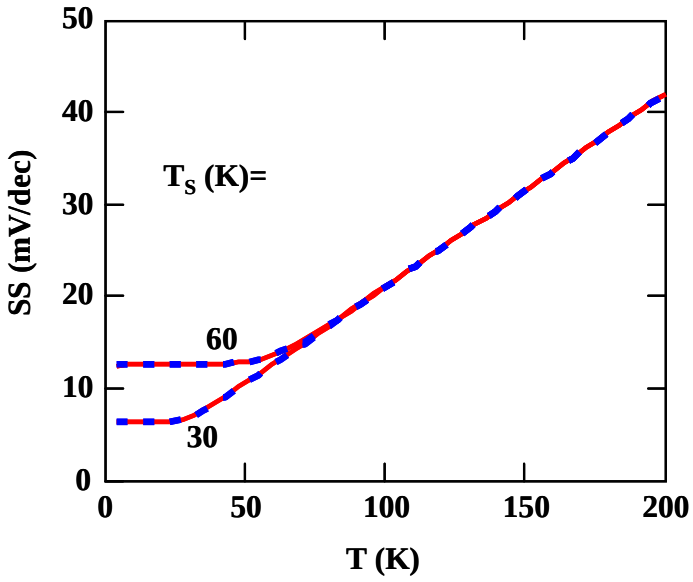

Fig. 2. Temperature dependence of subthreshold swing with temperature for various band tail width as given by Eq. (5) (red solid line) and analytical model of Eq. (7) (blue dashed line). $C_{ox}+C_d+C_{it})/C_{ox}=1.06$.

To underline the usefulness of Eq. (7), we have fitted the experimental results of SS(T) taken from Refs [8,9] and extracted the band tail extension temperature T_S as shown in Fig. 3. Depending on technology, this temperature lies typically in the range 30K to 50K.

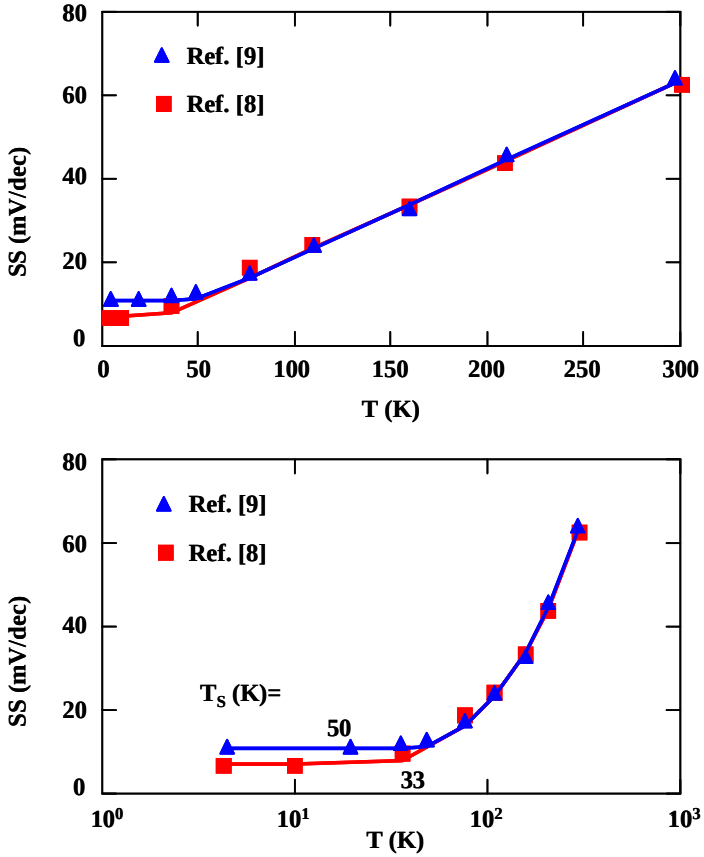

Fig. 3. Temperature dependence of subthreshold swing SS(T) as obtained from experiment (symbols) and modeling (solid line, Eq. 7) (Data from Refs [8,9], $(C_{ox}+C_d+C_{it})/C_{ox}=1.06$).

2.2. Conductivity approach

In section 2.1, we assumed that the drain current was proportional to the carrier density. Actually, this assumption is simplistic and certainly not valid at low temperature when the statistics becomes degenerate. In this case, the transport in the 2D subband inversion layer could be rather evaluated using the Kubo-Greenwood formalism [11,12]. In general, the macroscopic sheet conductivity is thus given by [11,12]:

$$\sigma(T,E_f)=\int_{-\infty}^{+\infty}\sigma_E(E).\left(-\frac{\partial f}{\partial E}(E,E_f)\right)dE \tag{8}$$

where $\sigma_E(E)$ is the energy conductivity function, which is related to the mobility function by the Cohen's formula [13],

$$\mu(E)=\frac{1}{qN(E)}.\frac{d\sigma_E(E)}{dE} \tag{9}$$

If we assume that the mobility function is constant, $\mu(E)=\mu_0$, and that the density of states features an exponential tail as given by Eq. (2), the conductivity function can thus be obtained after integration of Eq. (9) in the form,

$$\sigma_E(E,\Delta E) = q.A_{2D}.\mu_0.\Delta E.Ln(1+e^{E/\Delta E}) \tag{10}$$

In this situation, it should be noted that the conductivity function of Eq. (10) plays the role of the density of states of Eq. (2) in the carrier density approach. As can be seen in Fig. 4, it exhibits an exponential tail as a function of energy associated to that of the band density of states below the band edge (E<0). Note also that, as is usual, $\sigma_E(E)$ increases with energy above the band edge due to the increase of the carrier kinetic energy [11,12,14].

For a MOSFET and within the gradual channel approximation, the drain current constant along the channel reads $I_d=W.\sigma(T,E_f).(dE_f/dx)/q$, such that after integration over space x between source and drain, one gets,

$$I_d = \frac{W}{qL}\int_{E_{fS}}^{E_{fD}}\left[\int_{-\infty}^{+\infty}\sigma_E(E).\left(-\frac{\partial f}{\partial E}(E,E_f)\right)dE\right]dE_f \tag{11}$$

yielding after some manipulation,

$$I_d = \frac{W}{qL}\left[\int_{-\infty}^{+\infty}\sigma_E(E).f(E,E_{fS})dE - \int_{-\infty}^{+\infty}\sigma_E(E).f(E,E_{fD})dE\right] \tag{12}$$

where E_{fS} and $E_{fD}=E_{fS}-qV_d$ are the Fermi level at source and drain, respectively, and V_d the drain voltage.

Proceeding as in section 2.1 for Eqs (3)-(5), one obtains for the subthreshold swing in weak inversion,

$$SS(T) = \frac{1}{q}.\frac{\int_{-\infty}^{+\infty}\sigma_E(E).f(E,E_{fS})dE - \int_{-\infty}^{+\infty}\sigma_E(E).f(E,E_{fD})dE}{\int_{-\infty}^{+\infty}\sigma_E(E).\left(-\frac{\partial f}{\partial E}(E,E_{fS})\right)dE - \int_{-\infty}^{+\infty}\sigma_E(E).\left(-\frac{\partial f}{\partial E}(E,E_{fD})\right)dE}.\frac{C_{ox}+C_d+C_{it}}{C_{ox}} \tag{13}$$

Note the similarity between Eq. (5) and Eq. (13) for the subthreshold swing. In the saturation region of weak inversion i.e. when $Vd>>kT_S/q$ or $Vd>>kT/q$, the drain terms in Eqs (12) and (13) is cancelling out such that the subthreshold swing reduces to,

$$SS(T) = \frac{1}{q}.\frac{\int_{-\infty}^{+\infty}\sigma_E(E).f(E,E_{fS})dE}{\int_{-\infty}^{+\infty}\sigma_E(E).\left(-\frac{\partial f}{\partial E}(E,E_{fS})\right)dE}.\frac{C_{ox}+C_d+C_{it}}{C_{ox}} \qquad \text{(saturation)} \tag{14}$$

In this situation, the conductivity function lies in the band tail, so that, $\sigma_E(E,\Delta E) \approx q.A_{2D}.\mu_0\Delta E.e^{E/\Delta E}$, and thus is proportional to N(E,ΔE), implying perfect equivalence

between Eq. (5) and Eq. (14) for the subthreshold swing. However, note that this is only true because a constant mobility function $\mu(E)=\mu_0$ has been assumed. In general, there is no reason for the mobility function to be constant with energy, especially in the band tail where activated transport in localized states might occur as discussed in [11,15]. Therefore, Eq. (13) should constitute the most general expression for the subthreshold swing in a MOSFET. As for Eq. (5), it can be very well fitted by the analytical formula of Eq. (7), enabling the extraction of T_S from the SS cryogenic saturation level, $(kT_S/q).(C_{ox}+C_d+C_{it})/C_{ox}$), and, by turn, ΔE the band tail extension in terms of conductivity function and not necessarily in terms of density of states.

Fig. 5 compares the temperature dependence of the subthreshold swing as given by the carrier density approach (Eq. (5)) and the conductivity approach (Eq. (13)) calculated with the same band tail extension (here ΔE=5meV i.e. $T_S \approx 60$K). As already mentioned above, in this case, the two approaches are perfectly equivalent and give the same result. Indeed, in the case where the band tail extension for the conductivity function were different from that of the DOS, the curves would be distinct. Nevertheless, it is worth mentioning that, in practice, since the SS is measured from the drain current variation, it means that the extracted band tail does correspond to that of the conductivity function. The band tail extension for the DOS could only be extracted from the direct measurement of the carrier density (e.g. from integration of gate-to-channel capacitance vs V_g) as a function of gate voltage in weak inversion. But, this type of capacitive measurements should not have the sufficient dynamic range to extract precisely the band tail extension from the derivative of $n(V_g)$ curves.

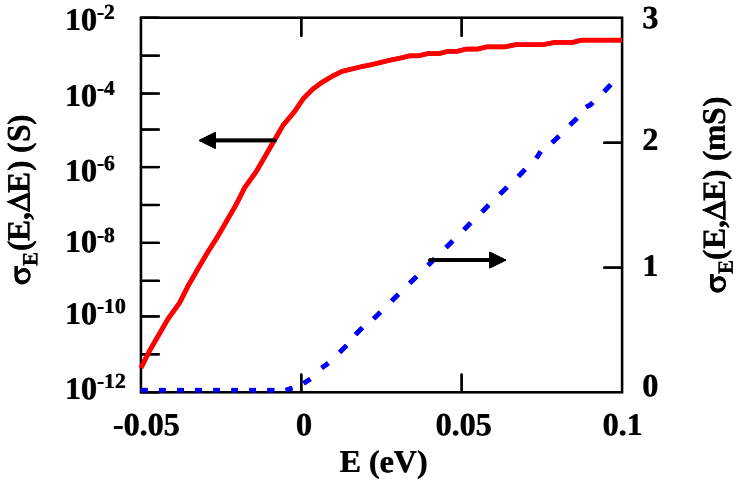

Fig. 4. Conductivity function $\sigma_E(E)$ with exponential tail (E=0 corresponds to band edge, ΔE=3meV, μ_0=1000cm^2/Vs).

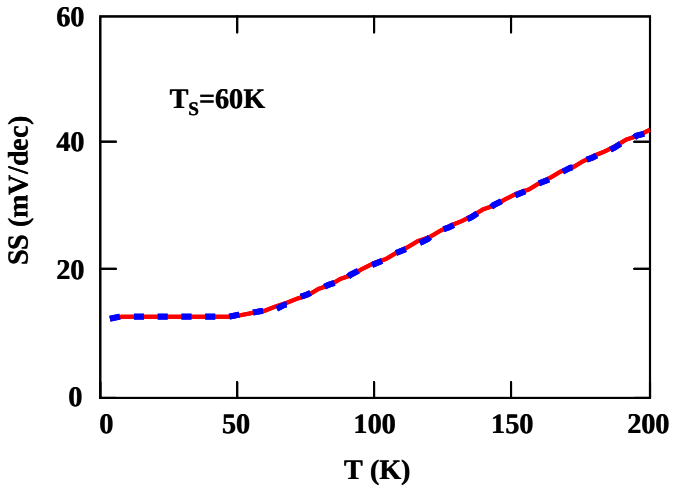

Fig. 5. Temperature dependence of subthreshold swing with temperature as given by carrier density approach Eq. (5) (red solid line) and conductivity approach Eq. (13) (blue dashed line) using the same band tail width ΔE=5meV.

3. Conclusion

We have first proposed a comprehensive analysis of the MOSFET subthreshold swing for a 2D subband with exponential band tail of states. We then derived a compact analytical expression for the subthreshold swing as a function of temperature, which well accounts for both its cryogenic temperature saturation and classical higher temperature increase. Moreover, we have generalized the subthreshold swing calculation to the more realistic situation where the transport and, by turn, the MOSFET drain current should be evaluated from the conductivity function (and not simply from the carrier DOS) within the Kubo-Greenwood formalism.

Acknowledgment

This work was partially supported by EU H2020 RIA project SEQUENCE.

References

1. A. Kamgar, Subthreshold behavior of silicon MOSFETs at 4.2 K, Solid-State Electron., 25, 537–539 (1982).
2. E. A. Gutierrez-D, J. Deen, and C. Claeys, Low Temperature Electronics: Physics, Devices, Circuits, and Applications (Elsevier, 2000).
3. F. Balestra and G. Ghibaudo, Device and circuit cryogenic operation for low temperature electronics (Kluwer, Boston, 2001).
4. T. Wada, H. Nagata, H. Ikeda, Y. Arai, M. Ohno, ·K. Nagase, Development of low power cryogenic readout integrated circuits using fully-depleted-silicon-on-insulator CMOS technology for far-infrared image sensors, J. Low Temp. Phys., 167, 602–608 (2012).
5. R. M. Incandela, L. Song, H. Homulle, E. Charbon, A. Vladimirescu, F. Sebastiano, Characterization and Compact Modeling of Nanometer CMOS Transistors at Deep-Cryogenic Temperatures, IEEE Journal of the Electron Devices Society, 6, 996-1006 (2018).
6. J.M. Hornibrook, et al., Cryogenic control architecture for large-scale quantum computing, Phys. Rev. Applied, 3, 024010 (2015).
7. R. Maurand, X. Jehl, D. Kotekar-Patil, A. Corna, H. Bohuslavskyi, R. Lavieville, L. Hutin, S. Barraud, M. Vinet, M. Sanquer and S. De Franceschi, A CMOS silicon spin qubit, Nat. Commun., 7, 13575 (2016).
8. H. Bohuslavskyi, A. G. M. Jansen, S. Barraud, V. Barral, M. Cass´e, L. Le Guevel, X. Jehl, L. Hutin, B. Bertrand, G. Billiot, G. Pillonnet, F. Arnaud, P. Galy, S. De Franceschi, M. Vinet, and M. Sanquer, Cryogenic Subthreshold Swing Saturation in FD-SOI MOSFETs described with Band Broadening, IEEE Electron Device Letters, 40, 784-787 (2019).
9. A. Beckers , F. Jazaeri , and C. Enz, Theoretical Limit of Low Temperature Subthreshold Swing in Field-Effect Transistors, 41, 276-279 (2020).
10. E. Arnold, Disorder-induced carrier localization in silicon surface inversion layers, Appl. Phys. Lett. 25, 705 (1974).
11. N. F Mott and E. A Davis, Electronic Processes In Non-crystalline Materials (Oxford, Clarendon, 1979)
12. G. Ghibaudo, Transport in the inversion layer of a MOS transistor: use of Kubo-Greenwood formalism, Journal of Physics C: Solid State Physics, 19, 767-780 (1986).
13. M. H. Cohen, E. N. Economou, and C. M. Soukoulis, Microscopic mobility, Phys. Rev. B 30, 4493-4500 (1984).
14. J.S. Dugdale, The electrical properties of metals and alloys (London, Arnold, 1977)
15. G. Ghibaudo, Analysis of the Hall effect in the localised states below the mobility edge, Journal of Physics C: Solid State Physics, 20, L769-L773 (1987)